RSC Advances

ROYAL SOCIETY OF CHEMISTRY

www.rsc.org/advances

Cite this: DOI: 10.1039/c0xx00000x

www.rsc.org/xxxxxx

ARTICLE TYPE

Solvothermal Synthesis of Magnetic Copper Nitride Nanocubes with Highly Electrocatalytic Reduction Properties

Pinxian Xi,[ab] Zhihong Xu,[a] Daqiang Gao,[c] Fengjuan Chen,[b] Desheng Xue,[c] Chun-Lan Tao,*[d] and Zhong-Ning Chen*[a]

Received (in XXX, XXX) Xth XXXXXXXXX 20XX, Accepted Xth XXXXXXXXX 20XX
DOI: 10.1039/b000000x

This study reports a successful solvothermal approach to synthesize copper nitride (Cu_3N) nanocubes. Magnetic measurements indicate that the fabricated Cu_3N nanocubes exhibit room temperature ferromagnetism and excellent electrocatalytic activity toward oxygen reduction reaction (ORR) and nitrobenzene reduction (NBR).

Nobel metal free nanomaterials exhibit many unique properties, and are thus attractive materials for numerous applications.[1] Copper nitrides are important band-gap semiconductors with a narrow band gap (1.2-1.6 eV) and have been commercialized as promising materials in optical storage devices,[2] high-speed integrated circuits,[3] and microscopic metal links.[4] However, extensive research on Cu_3N films, focusing on the solvothermal synthesis and electrocatalytic properties of shaped cubic nanocrystals, has been less conducted.[5] In most cases, traditional high-temperature synthetic methods yield products with minimal surface areas because significant sintering occurs at high temperatures. We therefore hypothesized that low temperature synthesis should be favoured for the applications to obtain broader surface areas.[6]

Recently, a new magnetic phenomenon, d^0 ferromagnetism (FM), has attracted significant attention in magnetic semiconductors, where the magnetic properties of the materials are not exclusively related to the presence of magnetic ions but can be strongly determined by the defects.[7] Defect-related FM has been reported in pure metal oxides such as ZnO, MgO, CaO, Al_2O_3, CeO_2, and MoO_2 (films, powders, etc.).[7] Moreover, previous studies have identified defect deduced FM in other systems, except for oxide dielectrics, including CaB_6,[8] GaN,[9] NbN,[10] thereby suggesting their potential application in spintronics.[11] Furthermore, extending the new d^0 ferromagnetism material system opens a new approach to explore the spintronics found in pristine lower-dimensional nanostructures.

It is known that promoting the oxygen reduction reaction (ORR)[12] at the cathode is an important step toward building fuel cells or metal-air batteries into highly efficient energy conversion devices.[13] ORR is always observed at a more negative potential due to the difficulty of O_2 adsorption on electrode surfaces and O-O bond activation/cleavage/oxide removal. Nitrobenzene (NB) is a highly toxic and refractory compound widely used in the preparation of different types of products such as dyes, explosives and pesticides. It is a highly hazardous substance because of its mutagenicity, recalcitrance and accumulation in the environment. The elimination of NB from the environment is highly challenging.[14] Herein, we report a simple and effective procedure to synthesize d^0 ferromagnetism cubic Cu_3N nanocrystals at temperatures below 300 °C, using 1-octadecylamine (ODA) and oleylamine (OAm) as solvents. These Cu_3N nanocubes also manifest high electrocatalytic activity towards both the oxygen reduction reaction (ORR) and nitrobenzene reduction (NBR).

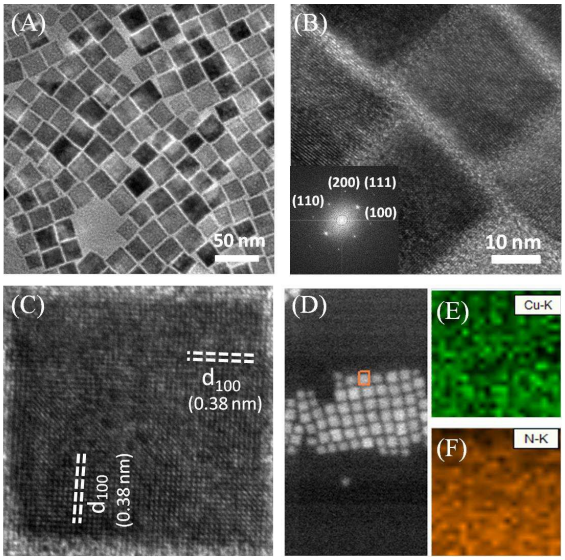

Fig.1 (A) Low-resolution TEM image. (B, C) HRTEM images at different magnifications. The inset of (B) shows a SAED pattern of the Cu_3N nanocubes. (D) HAADF STEM image of the Cu_3N nanocubes, and the corresponding elemental mapping for (E) Cu, and (F) N.

Cubic Cu_3N nanocrystals were synthesized in organic solvents through a solvothermal process. Copper (II) nitrate was dissolved in a mixed solvent of ODA and OAm. The reaction solution was first degassed at 110 °C for 1 h under a flow of nitrogen, and subsequently heated to 240 °C and then maintained at this temperature for 10 min. During the

reaction, the colour of the solution changed from blue to green, and finally to yellow. The Cu_3N nanocubes were obtained by centrifugation and purification (see ESI for details). Detailed growth process of these Cu_3N nanocubes with different reaction times can be illustrated in three stages including (i) nucleation stage to form nanoparticles, (ii) growth stage with the nanoparticles growth to nanocubes as a result of surface tension effects of the solvents, and (iii) molding stage with uniform nanocubes formed. The proposed growth procedure had been shown in Fig. S2 (ESI).

The overall morphology of the nanocrystals is characterized by uniform cubic shape without impurity particles or aggregates. Fig. 1A reveals a transmission electron microscopy (TEM) image of the Cu_3N nanocrystals, synthesized in the mixed solution of ODA and OAm. Fig. 1B and C display high-resolution TEM (HRTEM) images at different magnifications, from which the highly crystalline nanocubes with well resolved lattice fringes can be observed. Polycrystalline features were observed from the selected-area electron diffraction (SAED) pattern (Fig. 1B, inset). The fringes with interplanar spacing of 3.8 Å can be indexed as the (100) plane Cu_3N. To obtain further insight into the distribution of Cu and N in the as-synthesized Cu_3N nanocubes, elemental analysis was carried out with scanning transmission electron microscopy (STEM). Fig. 1D shows a high-angle annular dark-field (HAADF) micrograph of a selected area of the Cu_3N nanocubes. From the elemental maps of Cu and N and their overlay (Fig.1E and F), we can conclude that Cu and N are evenly distributed in the Cu_3N nanocubes.

The crystal structure of the Cu_3N nanocubes was further examined with X-ray techniques. The diffraction peaks of the prepared Cu_3N nanocrystal XRD pattern (Fig. S1A, ESI) could be indexed to the (100), (110), (111), (200), (210), (211), (220), and (300) planes of Cu_3N. All of the diffraction peaks agree well with the standard diffraction data for bulk Cu_3N (JCPDS No.47-1088). The oxidation states of Cu and N were also investigated with X-ray photoelectron spectroscopy (XPS). The Cu 2p and N 1s XPS spectra of the sample are depicted in Fig. S1B, C and D (ESI). The strong peaks at ~933.8 and 952.6 eV can be ascribed to the binding energies of the $2p^{3/2}$ and $2p^{1/2}$ electrons of Cu(I).

The magnetizations versus magnetic field (*M-H*) curves of the Cu_3N nanocubes, measured at different temperatures, are presented in Fig. 2A. It is indicated that these curves are composed of two parts. At lower fields (H < 1600 Oe), the curves exhibit clear magnetic hysteresis and behave as a paramagnetic system at higher fields (H>1600 Oe). After subtracting the paramagnetic component, the clear S-shape saturated open curves are observed for all the measured temperatures with the saturation magnetization (M_s) of 0.0043 emu/g at room temperature, revealing the room temperature ferromagnetic properties of the Cu_3N nanocubes. Furthermore, it can be seen in Fig. 2C that both the coercivity (H_c) and the M_s decrease, from 115 to 44 Oe and from 0.0063 to 0.0043 emu/g monotonically with the increase of the temperature, revealing a typical signature of nominal FM-like material.[15] The zero-field-cooled (ZFC) and field-cooled (FC) magnetization curves at the dc field of 100 Oe on the sample are shown in the inset of Fig. 2B, where The ZFC result shows no blocking temperature in the range of 5 to 300 K, implying that there is no ferromagnetic contamination in the sample. The FC curve exhibits an obvious deviation from the ZFC curve until the temperature exceeds 300 K, indicating that the Curie temperature of the sample is expected to exceed 300 K. The magnetization versus temperature (*M-T*) curve was measured in the range of 5-300 K at 8000 Oe to further explore the ferromagnetism of the sample (Fig. 2D). This curve shows a rapid decay of magnetization, at the low temperature region, with the increase of the temperature. Subsequently, the magnetization declines gradually but does not go to zero until 300 K, indicating a PM phase mixed with a FM phase for the sample. The *M-T* curve is fitted by the $T^{3/2}$ law for FM phase and the Curie-Weiss law for PM phase, as shown by the following equation[16]

$$M(T) = M_{s0}(1 - AT^{3/2}) + CH/T \quad (1)$$

where M_{s0} is the saturation magnetization at T = 0 K, A is a coefficient correlated to the structure and properties of the materials, and C is the Curie constant. As shown in Fig. 2D, the PM and FM part as well as the total magnetization are plotted separately, in which the total simulation from Eq. 1 gives a good fitting of the experimental results. These results indicate that the fabricated Cu_3N nanocubes belong to the material systems of d^0 ferromagnetism, resulting from the surface defects.[17]

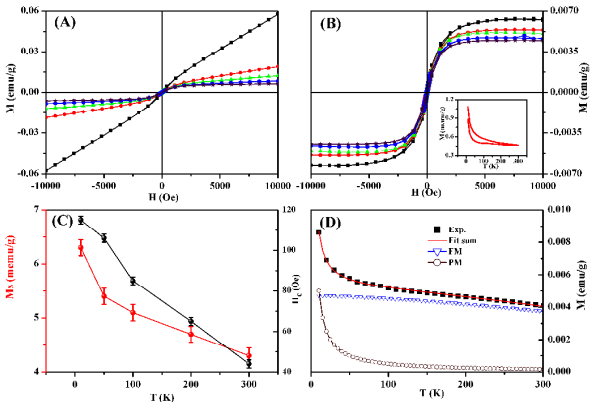

Fig.2 (A) Original *M-H* curves for the Cu_3N nanocubes measured at different temperatures. (b) *M-H* curves for the Cu_3N nanocubes after deducting the paramagnetic signal. Inset represents the corresponding FC and ZFC curves. (c) Dependence of M_s and H_c on the measured temperatures for the Cu_3N nanocubes. (D) *M-T* curve of the Cu_3N nanocubes in the range of 5-300 K at 8000 Oe.

The electrocatalytic activity of the unsupported Cu_3N nanocubes was evaluated through electrochemical measurements by depositing 3.3 μg of the crystals on a glassy carbon electrode (referred to as Cu_3N/GC). Fig. 3A shows the CVs of the Cu_3N nanocubes in a 0.1 M solution of KOH saturated with either nitrogen or oxygen at a potential scan rate of 0.1 V s^{-1}. Compared to the featureless CV profile in the N_2 saturated electrolyte, a strong reduction current peak is observed when the electrolyte is saturated with O_2, suggesting that the O_2 is quite easily reduced on Cu_3N nanocubes owing to its high ORR activity. The electrochemical reduction performance of the Cu_3N nanocubes was also tested for

nitrobenzene reduction. The peak current of Cu_3N nanocubes modified electrodes for NB is boosted significantly, meanwhile the potential shows 140 mV anodic shift compared to bare GCE. Noteworthily, the electrocatalytic activity of the sample towards NBR is comparable to commercial Pd/C, indicating that Cu_3N nanocubes prepared in this study exhibit a high NBR electrocatalytic activity. The cyclic voltammogram summarizing the catalytic performance of Cu_3N nanocubes under different scanning rates is presented in Fig.3B. Differential Pulse Voltammetry (DPV) was employed to evaluate the behaviour of nitrobenzene reduction for bare GCE, Pd/C and Cu_3N nanocube modified electrodes under identical conditions with 0.5 mM NB containing 0.5 M KCl and 0.2 M PBS (pH = 7), as depicted in Fig. 3C and the NBR of Cu_3N at different concentrations is illustrated in Fig.3D. The signal shows linear correlation between the concentration of NB and the peak current in the range from 0 to 300 ppm, with a correlation coefficient of R = 0.990 (Fig. S3, ESI), from which the detection limit of 0.48 ppm at S/N = 3 is estimated. The lower detection limit and wider linear range (Fig.S4, ESI) imply that Cu_3N nanocubes present excellent NBR electrocatalytic activity.

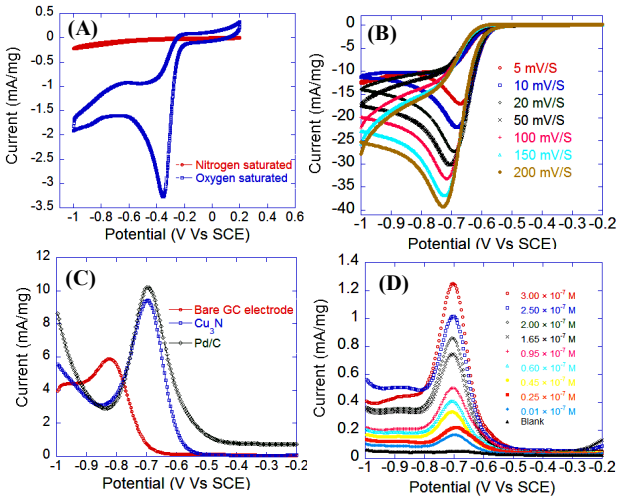

Fig. 3 (A) CVs of Cu_3N nanocubes supported on glassy carbon substrate in N_2 or O_2 saturated 0.1 M KOH solution. Potential scan rate, 0.1 V s^{-1}. (B) Cyclic voltammograms of Cu_3N nanocubes modified electrode in 0.5 mM NB containing 0.2 M PBS and 0.5 M KCl electrolyte at different scanning rates. (C) Differential pulse voltammograms of Cu_3N and Pd/C modified electrode in 0.5mM NB containing 0.2M PBS and 0.5M KCl. (D) Differential pulse voltammograms for different concentrations of NB containing 0.2 M PBS and 0.5 M KCl at Cu_3N nanocubes modified electrode.

In summary, we have demonstrated a facile single-phase process to synthesize cubic Cu_3N nanocubes. The synthesized Cu_3N nanocubes exhibit magnetic hysteresis loop and prominent ferromagnetic resonance signals at ambient temperature. The Cu_3N nanocubes also exhibit electrocatalytic activity towards ORR and NBR in electrochemical studies. The relatively low detection limit of the Cu_3N nanocubes for NB identifies these materials as promising electrochemical sensors.

This work was supported by the NSFC (Nos. 21201092, 51202101, U1304202), the Research Fund for the Doctoral Program of Higher Education (Nos. 20120211120020, 20120211120005), the Gansu NST (1208RJYA028) and the Fundamental Research Funds for the Central Universities (Lzujbky-2012-65) and (Lzujbky-2013-194).

Notes and references

[a]*State Key Laboratory of Structural Chemistry, Fujian Institute of Research on the Structure of Matter, Chinese Academy of Sciences, Fuzhou, Fujian 350002, P. R. China*
E-mail: czn@fjirsm.ac.cn..
[b]*Key Laboratory of Nonferrous Metal Chemistry and Resources Utilization of Gansu Province, State Key Laboratory of Applied Organic Chemistry and Colleague of Chemistry and Chemical Engineering, Lanzhou University, Lanzhou, 730000, P. R. China.*
Fax: +86 931 8912582; Tel: +86 931 8912589
[c]*Key Laboratory for Magnetism and Magnetic Materials of MOE, Lanzhou University, Lanzhou, 730000, P. R. China.*
[d]*School of Physcial Science and Technology, Lanzhou University, Lanzhou 730000, P. R. China.*
E-mail: taochl@lzu.edu.cn.

† Electronic Supplementary Information (ESI) available: [details of any supplementary information available should be included here]. See DOI: 10.1039/b000000x/

‡ Footnotes should appear here. These might include comments relevant to but not central to the matter under discussion, limited experimental and spectral data, and crystallographic data.

1. Y. Du, Z. Yin, J. Zhu, X. Huang, X. Wu, Z. Zeng, Q. Yan, H. Zhang, *Nat. Commun.*, 2012, **3**, 1177.
2. (a) H. Wu, W. Chen, *J. Am. Chem. Soc.*, 2011, **133**, 15236. (b) P. Lignier, R. Bellabarba, R. P. Tooze, *Chem. Soc. Rev.*, 2012, **41**, 1708. (c) L. Hung, C. Tsung, W. Huang, P. Yang, *Adv. Mater.*, 2010, **22**, 1910.
3. D. M. Borsa, S. Grachev, C. Presura, D. O. Boerma, *Appl. Phys. Lett.* 2002, **80**, 1823.
4. D. M. Borsa, D. O. Boerma, *Surf. Sci.* 2004, **548**, 95.
5. (a) D. Wang, Y. Li, *Chem. Commun.*, 2011, **47**, 3604. (b) 1a
6. (a) C. H. Jaggers, J. N. Michaels, A. M. Stacy, *Chem. Mater.*, 1990, **2**, 150. (b) 4a.
7. D. Gao, G. Yang, J. Li, J. Zhang, J. Zhang, D. Xue, *J. Phys. Chem. C* 2010, **114**, 18347.
8. D. J. Shang, K. Yu, Y. S. Zhang, J. W. Xu, J. Wu, Y. Xu, L. J. Li, and Z. Q. Zhu, *Appl. Surf. Sci.* 2009, **255**, 4093.
9. C. Madhu, A. Sundaresan, and C. N. R. Rao, *Phys. Rev. B*, 2008, **77**, 201306(R) .
10. Shipra, A. Gomathi, A. Sundaresan, and C. N. R. Rao, *Solid State Commun.*, 2007, **142**, 685 .
11. (a) Z. Németh, K. Nomura, Y. Ito, *J. Phys. Chem. C*, 2009, **113**, 20044. (b) L. Li, R. Qin, H. Li, L.Yu, Q. Liu, G. Luo, Z. Gao, J. Lu, *ACS Nano*, 2011, **5**, 2601.
12. (a) S. Guo, S. Zhang, S. Sun, *Angew. Chem. Int. Ed.*, 2013, **52**, 8526. (b) Y. Dong, Y.Wu, M. Liu, J. Li, *Chem Sus Chem*, 2013, **6**, 2016. (c) M. Liu, Y. Dong, Y. Wu, H. Feng, J. Li, Chem. Eur. J., 2013, **19**, 14781. (d) H. Zhu, S. Zhang, S. Guo, D. Su, S, Sun, *J. Am. Chem. Soc.*, 2013, **135**, 7130.
13. (a) M. Winte, R. J. Brodd, *Chem. Rev.*, 2004, **104**, 4245. (b) A. A. Gewirth, M. S. Thorum, *Inorg. Chem.*, 2010, **49**, 3557. (c) C. Wang, H. Daimon, T. Onodera, T. Koda, Sun, S. *Angew. Chem., Int. Ed.*, 2008, **47**, 3588.
14. X. Lu, H. Qi, X. Zhang, Z. Xue, J. Jin, X. Zhou, X. Liu, *Chem. Commun.*, 2011, **47**, 12494.
15. D. Q. Gao, J. Y. Li, Z. X. Li, Z. H. Zhang, J. Zhang, H. G. Shi, D. S. Xue, *J. Phys. Chem. C*, 2010, **114**, 11703 .
16. (a) K. M. Hanif, R. W. Meulenberg, and G. F. Strouse, *J. Am. Chem. Soc.*, 2001, **124**, 11495. (b) K. Mitchell, F. Q. Huang, A. D. McFarland, C. L. Haynes, R. C. Somers, R. P. Van Duyne, J. A. lbes, *Inorg. Chem.*, 2003, **42**, 4109.
17. D. Gao, G. Yang, J. Zhang, Z. Zhu, M. Si, and D. Xue, *Appl. Phys. Lett.*, 2011, **99**, 052502.

Graphic Abstract

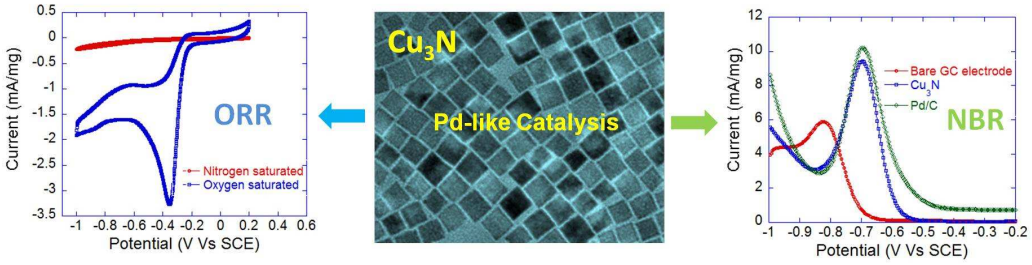

Copper nitride (Cu_3N) nanocubes prepared by organic solvothermal approach exhibit excellent electrocatalytic activity toward oxygen reduction reaction (ORR) and nitrobenzene reduction (NBR).